SILAR deposition of Ni(bpy)3X: X = (NCS)2, (Fe(CN)5NO), and (Ag(CN)2)2 thin films on glass substrates

Hacene Bendjeffal, D. Guibedj, Guillaume Chastanet, Jean François Létard, F. Djazi, Azzedine Abbaci, Kamel Guerfi, Yacine Abdelkader Bouhedja

▶ **To cite this version:**

Hacene Bendjeffal, D. Guibedj, Guillaume Chastanet, Jean François Létard, F. Djazi, et al.. SILAR deposition of Ni(bpy)3X: X = (NCS)2, (Fe(CN)5NO), and (Ag(CN)2)2 thin films on glass substrates. Synthesis and Reactivity in Inorganic, Metal-Organic, and Nano-Metal Chemistry, 2016, 46 (12), pp.1741-1750. 10.1080/15533174.2015.1137055 . hal-01383694

HAL Id: hal-01383694
https://hal.science/hal-01383694v1

Submitted on 2 Mar 2021

HAL is a multi-disciplinary open access archive for the deposit and dissemination of scientific research documents, whether they are published or not. The documents may come from teaching and research institutions in France or abroad, or from public or private research centers.

L'archive ouverte pluridisciplinaire **HAL**, est destinée au dépôt et à la diffusion de documents scientifiques de niveau recherche, publiés ou non, émanant des établissements d'enseignement et de recherche français ou étrangers, des laboratoires publics ou privés.

SILAR deposition of $Ni(bpy)_3X$: { X = $(NCS)_2$, $(Fe(CN)_5NO)$ and $(Ag(CN)_2)_2$} thin films on glass substrates

H. Bendjeffal[1], D. Guibedj[1], G. Chastanet[2], J-F.Letard[2], F. Djazi[3], A. Abbaci [1], K. Guerfi [1] Y.Bouhedja[1] *

[1.] Department of chemistry, Badji Mokhtar University, BP 12, Annaba 23000, Algeria.
[2.] ICMCB,CNRS, University Bordeaux (I), 33608 Pessac Cedex, France
[3.] Department of chemistry, University, Skikda 21000, Algeria.

Corresponding authors*: Yacine Bouhedja Department of chemistry, Badji Mokhtar University, BP 12, Sidi Amar Annaba 23000, Algeria. E-mail: ybouhadja@yahoo.fr

.

Abstract

The present study is focuses on the preparation of thin layers based on hybrid materials (organometallic complexes) deposited onto glass substrates. The deposition experiments of $[Ni(bpy)_3](NCS)_2$, $[Ni(bpy)_3](Ag(CN)_2)_2$ and $[Ni(bpy)_3](Fe(CN)_5NO)$ were performed on glass slides (18 mm x 18 mm) by SILAR method (Successive Ionic Layer Adsorption and Reaction). The influence of some parameters, such as dipping cycle's numbers (30, 60 and 120 dipping cycles), temperature (20°C, 30°C, 40°C and 50°C), precursor's concentration (10^{-3} , 10^{-2} and 10^{-1} M); and the nature of the counter-anions were studied. Different methods (UV-Vis, SEM, FTIR and XRD) were used to characterize the deposited layers in order to determine the absorption coefficient (α) and gap's energy (E_g) of the materials.

Keywords: Complexes, Ni(II), optical proprieties, SILAR, thin films.

1. Introduction

During the last decades, the development of thin layers containing a nanomaterial have had a great interest in the activities of the scientific research groups; they are the basic materials for many applications in nanotechnology and the subject of several studies which reported specially that for electronics, photomagnetism, catalysis, photovoltaic and optoelectronics…etc [1-10]. Indeed the thin layers can be prepared starting from various materials such as silicon, metallic oxides (ZnO, NiO and $NiCoO_x$ …etc.) [4-6], metallic sulfides (CdS, Cd-Zn-S…etc.) [7-9], alloys materials and organo-metal complexes of magnesium(II), calcium(II), zin(II), nickel(II), Cobalt(II), copper (II)…etc) [10-22].

One of the most promising strategies is based on thin films of nickel compounds (oxides, salts, complexes…etc.) development; sensitive to certain physical parameters variations (temperature, pressure and light…etc.). Such an approach has stimulated scientific activities in this field, due to their various proprieties (optical, catalytic, electrical…etc.) [4-6]. Although, several works related to nickel compounds, few of them make reference to the deposition and optical properties of Nickel complexes thin films studies [4-6,11, 22].

Several techniques are used for thin film formation of transition metals complexes deposited materials; these include electrochemical deposition, chemical bath deposition (CBD), Langmuir−Blodgett (LB), spin-coating, Successive Ionic Layer Adsorption and Reaction (SILAR)…etc. [3, 14]. However, the SILAR method is a simple technique, it can be proved very good homogeneity and thickness control of multilayer deposed materials [11-16].

In the present article we reports the optical properties study of thin layers complexes: $[Ni(bpy)_3](NCS)_2$, $[Ni(bpy)_3](Ag(CN)_2)_2$ and $[Ni(bpy)_3](Fe(CN)_5NO)$ deposed onto glass substrates using the successive ionic layer adsorption and reaction method (SILAR) [2,7,8,18]. The thin films Ni(II)-complexes have been growing under the effect of a some operating parameters, such as dipping cycles numbers (30, 60 and 120 dipping cycles),

solution's temperature (20 °C, 30 °C, 40 °C and 50 °C), precursor's concentration (10^{-3} , 10^{-2}, and 10^{-1} M).

In the aim to determine the optimal condition used to elaborate a light-sensitive thin films of Ni(II)-complexes with a simple and inexpensive technique (SILAR), various analysis techniques (UV-Vis, FTIR, MEB and DRX) were used to characterize several samples. For this reason, the UV-Vis absorption spectra were used to study the optical proprieties such as gap's energy (E_g) and absorption coefficient (α) in order to use this materials as a selective absorber in many areas (solar cell, optical filters ...etc).

2. Experimental section

For the preparation of the complexes solutions that are deposited onto glass substrates (optical microscope glass slides: 18mm x18mm), we have used the chemical ($NiSO_4.6H_2O$, KSCN, $K[Ag(CN)_2]$, $Na_2[Fe(CN)_5NO].2H_2O$ and the 2,2-bipyridine (bpy: $C_{10}H_8N_2$) as provided by Merck.

2.1. Cleaning procedure of substrates

The microscope glass slides were cleaned in an ultra-sonic bath with a commercial detergent during 10 min, and then rinsed with distilled water pursued by a dipping in acetone for another 10 min, the substrates were then washed with dichloromethane. Finally, the whole was dried in vacuum at 105 °C during 90 minutes. However, the SILAR technique was used for the deposed the thin layer films on the cleaned glass substrates.

2.2. Formation of complexes thin films via SILAR method

The cleaned glass substrate was dipped successively into a series of precursors solutions according to a well-defined deposition protocol as shown in Fig. 1, where the

substrate was immersed during 40 s in beaker "A" containing the cationic solution of the complex $[Ni(bpy)_3]^{+2}$, then rinsed with distilled water in beaker "B" about 10s, then immersed in the solution of counter-anion X^- ($(NCS^-$, $[Fe(CN)_5NO]^{-2}$, $[Ag(CN)_2]^-$) in beaker "C" during 40s, finally rinsed a second time with distilled water in a beaker “D”. The above procedure was repeated several times for many cycles. At the end of each deposition; the thin film complexes was dried in a vacuum at 105 °C for 5 min. The mechanism formation of $[Ni(bpy)_3]X$: ($X^- = NCS^-$, $[Fe(CN)_5NO]^{-2}$ and $[Ag(CN)_2]^-$) thin films onto glass surface can be illustrated by Fig. 1 and via the following reactions:

$$Ni^{+2}{}_{(aq)} + 3bpy_{(aq)} \rightarrow [Ni(bpy)_3]^{+2}{}_{(aq)} \quad (1)$$

$$[Ni(bpy)_3]^{+2}{}_{(aq)} + 2\ SCN^-{}_{(aq)} \rightarrow [Ni(bpy)_3](NCS)_{2\ (S)} \downarrow \quad (2)$$

$$[Ni(bpy)_3]^{+2}{}_{(aq)} + 2\ [Ag(CN)_2]^- \rightarrow [Ni(bpy)_3](Ag(CN)_2)_{2\ (S)} \downarrow \quad (3)$$

$$[Ni(bpy)_3]^{+2}{}_{(aq)} + [Fe(CN)_5NO]^{-2} \rightarrow [Ni(bpy)_3]Fe(CN)_5NO]_{(S)} \downarrow \quad (4)$$

This same deposition protocol was repeated to study the effect of various parameters such as (cycle’s numbers, temperature and precursor’s concentration); on the thickness growth of studied complexes thin films. At the end of each deposition, the weight of the as-deposed thin layers were weighed each time, also the thicknesses of the films were measured with a profilometer (Dektak 3030 Surface Profiler).

2.2.1.Effect of precursor's concentration on the thickness growth of complexes thin films

The optical absorption UV-Vis spectra of $[Ni(bpy)_3](NCS)_2$, $[Ni(bpy)_3](Fe(CN)_5NO)$ and $[Ni(bpy)_3](Ag(CN)_2)_2$ recorded at room temperature in the range of 200 nm - 800 nm are shown in Fig. 2. All of UV-Vis absorption spectrum contains a wide intense band at 240 nm. The spectral intensities for the observed bands in the absorption spectra of these samples,

which are expressed in terms of transition strengths, show that the intensities increase with increasing of the precursor's concentration (10^{-3} M, 10^{-2} M and 10^{-1} M) according to the thin films thickness evolution (Fig.2.(d)) measured with a profilometer (Dektak 3030 Surface Profiler). The best results have been obtained with a 10^{-2} M precursor's concentration at 20 °C and 120 dipping cycles with a good thickness as can be seen from Table 1 and Fig.2.(c).

2.2.2. Effect of cycle's numbers on thickness growth of complexes thin films

We have used a spectrophotometer (Techcomp double-beams UV-Vis (8500 Ltd-China) for recording the optical absorption spectra of $[Ni(bpy)_3](NCS)_2$, $[Ni(bpy)_3](Fe(CN)_5NO)$ and $[Ni(bpy)_3](Ag(CN)_2)_2$ thin layers in the range of 200 nm - 800 nm as shown in Fig. 3. The spectral intensities for the observed intense bands in the samples absorption spectra, deposed at room temperature 20 °C and 10^{-2} M of precursors concentration with various dipping cycles (30, 60 and 120 dipping cycles) show that the absorption intensities increase with increasing the dipping cycles number as shown in Fig. 3. This result is in good agreement with the thickness growth reported in Fig. 2(d). For all the studied complexes, the best deposition results were obtained after 120 dipping cycles where the studied samples displayed strong and broad UV spectral intensities. The different values are reported in Table 1.

2.2.3. Effect of temperature on thickness growth of complexes thin films

The effect of precursor's solutions temperature on the thickness of the deposed thin layers has been studied at the optimal precursors concentration and dipping cycle numbers (Table 1) under various temperatures (20 °C, 30 °C, 40 °C and 50 °C) using thermostatic batch JULABO Labortechnik H.D-7760 Seelbach / Germany. The variation of thickness of the obtained complexes thin films was inspected by UV-Vis absorption spectrophotometry ;

the absorption spectra given in Fig. 4 (a, b and c), show that the temperature increase has a destructive action on the growth of all studied Ni(II)-complexes thin films, this observation is in accord with evolution of their respective thickness Fig. 4(d). Table 1 presents the optimal conditions, weight, thickness, and maximal absorption values of all studied complexes thin films.

2.3. Complexes thin films characterizations

2.3.1. Infrared analyses

The most important aspects concerning the Infrared (FTIR) spectra of the cyano organometallic complexes deal with the cyano vibration band (υ_{-CN}) in the region (2200 cm^{-1} - 1900 cm^{-1}). The appearance investigation of the (υ_{-CN}) has been realized using an infrared spectrometer (Shimadzu FTIR-8700 FT-IR spectrometer). The FTIR spectra of the deposed complexes layers which grows in optimal condition (20 °C, 120 dipping cycles and 10^{-2} M) are given in the Fig. 5. The infrared spectra of $[Ni(bpy)_3](NCS)_2$, $[Ni(bpy)_3](Ag(CN)_2)_2$ and $[Ni(bpy)_3](Fe(CN)_5NO)$ films show vibration bands respectively at 2090 cm^{-1}, 2180 cm^{-1} and 2200 cm^{-1} corresponding to cyano-vibration band (υ_{-CN}) characteristics of this materials. Moreover, the $[Ni(bpy)_3](Fe(CN)_5NO)$ thin film FTIR specter shows another vibration band at 1900 cm^{-1} corresponding nitro function [23-24].

2.3.2. Structural study

In Fig. 6(a), (b) and (c), are presented the DRX patterns spectra of $[Ni(bpy)_3](NCS)_2$, $[Ni(bpy)_3](Fe(CN)_5NO)$ and $[Ni(bpy)_3](Ag(CN)_2)_2$ thin films obtained in optimal conditions. The DRX pattern for the obtained $[Ni(bpy)_3](NCS)_2$ film shown in two diffraction peaks are observed at 44.5° and 78° corresponding respectively to indexed planes : (111) and (220) that can be assigned to face-centered cubic structure (JCPDF# 04-0850). The DRX pattern of as-

deposed films of $[Ni(bpy)_3](Fe(CN)_5NO)$ is presented in Fig. 6(b); many diffraction peaks are observed : 29.5° 32°, 44.5 , 65° and 78° which corresponds to the polycrystalline structure with indexed plans of (111), (200) and (220) of fcc-Ni/Fe structure (JCPDS# 87-0721). The DRX pattern of $[Ni(bpy)_3](Ag(CN)_2)_2$ thin layer Fig. 6(c**)** presents the diffraction peaks at 38.5° , 44.5 , 65° and 78° corresponding to indexed plan of (111), (200), (220) and (311) attributed to polycrystalline Ni/Ag structure (JCPDF# 04-0783) [25-29].

2.3.3. Surface morphological studies

Scanning electron microscope (SEM) is known to be as one of the most important instrumentations in studying surface morphology of inorganic thin film by direct two dimensions surface imaging as well as possible determination of the average particle size [17]. Fig. 7 displays a typical SEM micrographs of the surface morphologies for $[Ni(bpy)_3]X$: (X= NCS^-, $[Fe(CN)_5NO]^{-2}$ and $[Ag(CN)_2]^-$) thin layers grows at 20 °C, 120 dipping cycle and 10^{-2} M. Moreover, Fig.7(a), (b) show that the surface of $[Ni(bpy)_3](SCN)_2$ and $[Ni(bpy)_3](Fe(CN)_5NO)$ films have a crystalline homogeneous microstructure with a particle size of the above 5µm. however the thin films of $[Ni(bpy)_3](Ag(CN)_2$ has a lower degree of crystalline with grain size is of the order of 3 µm.

2.4. Optical properties

UV-Vis spectrophotometry was used to study the optical properties such as light absorption, electronic transition, and optical band gap of Ni(II)-complexes thin films. The UV-Vis absorption spectra of the as-deposited thin films synthesized in optimal conditions Figs. 2 , 3 and 4, show that all Ni(II)-complexes thin films samples have a large and intense bands between (200 nm- 300 nm). It was found that the strong absorption bands observed in this area are mainly due to the principle types of electronic states transitions (d-d, d-π*, π-d π-

π* and n-π*) probable for organometallic complexes as reported by R.C. Evans et al [30], and M.E. Mahmoud et al [14]:

The coordination of ligand with metallic central atom effected the splitting of the "d" orbitals, which causes the "d-d " electronic transition. Excited d-d states started from promotion of an electron inside "d" orbital which are essentially confined to the metallic central atom . In the case of the "d-π*" states, the electronic transition are due to the charge transfer between the metallic central atom and ligand, These involve the excitation of a metal centered electron (d) to an the lowest unoccupied molecular orbital (π*) situated on the ligand molecule; while in the case of the "π-d" electronic transition, the charge transfer start from π bonding ligand system to the metal centered (d) orbital. In the case of "π-π*" or "n-π*" states, the electronic transitions are observed between ligand system orbitals; the promotion of an electron from a π-bonding or non-bonding orbital to the lowest unoccupied molecular orbital (π*) giving rise to these electronic transition [14, 30].

All studied Ni(II)-complexes thin layers have a maximal absorbance observed between 238 nm-241 nm) corresponding a π-π* or n-π* electronic transition between the highest occupied molecular orbital (HOMO) and the lowest unoccupied molecular orbital (LUMO) [14, 17, 30- 32]. The absorption coefficient and gap's energy has been the determined using the UV-Vis absorbance spectra of as-deposed thin layers synthesized in optimal conditions (120 cycles of dipping, 20° C and 10^{-2} M); the information about direct transitions was determined from the analysis of the spectral dependence of the absorption near the fundamental absorption edges within the framework of one electron [15,17]. The equation that relates the absorption coefficient α and the energy gap are given as [5,14]:

$$\alpha = (1 / d) \quad \ln (100 / T_{(\%)}) \tag{5}$$

$$\alpha (h\upsilon) = A (h\upsilon - E_g)^{1/2} \tag{6}$$

Where " T " is the transmittance (%), "α" is the absorption coefficient, "d" is thickness of thin films; the factor (A) depends on the transition probability assumed to be as constant within the optical frequency range, and E_g is the energy band gap value (eV) of the indicated transition. The extrapolation of the straight line graphs $[(\alpha h\upsilon)^2 = f(h\upsilon)]$ to zero absorption ($\alpha = 0$) provide the value of E_g. Figs. (8)-(10) display various plots of absorption coefficient (α) and $(\alpha h\upsilon)^2$ versus photon energy ($h\upsilon$) of the deposed complexes thin films.

This study shows that the gap's energy take the values of 3.0 eV, 3.4 eV and 4,6 eV for $[Ni(bpy)_3](NCS)_2$, $[Ni(bpy)_3](Fe(CN)_5NO)$ and $[Ni(bpy)_3](Ag(CN)_2])_2$ thin fims, respectively (Table 1). The obtained gaps energy values are simulated to results reported in the literature by M. A. Hussien et al [33-34], this study findings indicate that these complexes have the characteristics of semi-conductors. Moreover, the values of energy gaps belong to the range of highly efficient photovoltaic materials energies. Hence, the studied complexes can be considered as potential materials for many optical applications [30-34].

3. Conclusion

In this work, the thin films of $[Ni(bpy)_3](NCS)_2$, $[Ni(bpy)_3](Fe(CN)_5NO)$ and $[Ni(bpy)_3](Ag(CN)_2)_2$ were successfully deposed on glass slides using successive ionic layer adsorption and reaction method. The best deposition results were obtained after 120 cycle of dipping, with 10^{-2} M of precursor concentration (NCS^-, $[Fe(CN)_5NO]^{-2}$ et $[Ag(CN)_2]^-$) at 20°C. The as-deposed films were obtained in optimal conditions have thicknesses varied between 3,9 µm and 4,7 µm.

The scanning electronic microscope characterization show that as-deposited thin films have a crystalline microstructure with a grain size of the above of 5µm for $[Ni(bpy)_3](SCN)_2$)

and $[Ni(bpy)_3](Fe(CN)_5NO)$ samples and 3 µm for $[Ni(bpy)_3](Ag(CN)_2)_2$ film; also the DRX structural characterization show that the as-obtained complexes thin layers have polycrystalline.

The optical absorption analyses show that all studied complexes have strong in UV area (200 nm - 300nm) corresponding a π-π* or n-π* electronic transition between the highest occupied molecular orbital (HOMO) and the lowest unoccupied molecular orbital (LUMO), with various optical gap's energy varied between 3.0 eV and 4.6 eV.

References

[1] Kumar, L.M.M.D.; et al. Enhanced optical and electrical properties of Ni inserted ITO/Ni/AZO tri-layer structure for photoelectric applications. *Materials Science and Engineering B.* 2015, 195, 84-89.

[2] Farag, A.A.M.; and Haggag, S.M.S. Thin film assembly of nano-sized Zn(II)-8-hydroxy-5,7-dinitroquinolate by using successive ion layer adsorption and reaction (SILAR) technique: Characterization and optical-electrical-photovoltaic. *properties Spectrochimica Acta Part A.* 2012, 93, 116-124.

[3] Sohrabia, H.; Tabaiana, S.H.; Omidvara, H. Sajjadnejadb, M. Synthesis of Nanostructured TiO2 Coatings by Sol-Gel Method: Structural and Morphological Studies. *Synthesis and Reactivity in Inorganic, Metal-Organic, and Nano-Metal Chemistry*. DOI: 10.1080/15533174.2014.988231

[4] Farag, A.A.M.; and Mohamed, M.K.O. Structural and optical evaluations of deposited nanocrystalline NiO thin films via a Ni(II)–8-hydroxyquinolate complex by the static step-by-step soft surface reaction technique for optoelectronic applications. *Polyhedron.* 2014, 71, 75-84.

[5] Benzarouk, H.; Drici, Ab. Effect of different dopant elements (Al, Mg and Ni) on microstructural, optical and electrochemical properties of ZnO thin films deposited by spray pyrolysis (SP). *Superlattices and Microstructures.* 2012, 52, 594-604.

[6] Jung, C. H.; Lee, J. Y.; Pu, L. S.; and Yoon, D. H. Investigation on the Doping Dependence of Solution-Processed Zinc Tin Oxide Thin Film and Thin-Film Transistors. *Synthesis and Reactivity in Inorganic, Metal-Organic, and Nano-Metal Chemistry*. 201, 41, 1153-1157.

[7] Sun, H.; Mu, J. SILAR Deposition of CdS Thin Films on Glass Substrates Modified with 3-Mercaptopropyltrimethoxysilane. *Journal of Dispersion Science and Technology*. 2005, 26, 719-722.

[8] Nicolau, Y. F.; and Menard, J. C. Solution growth of ZnS, CdS and $Zn_{1-x}Cd_xS$ thin films by the successive ionic-layer adsorption and reaction process. *growth mechanism journal of crystal growth.* 1988, 92,128-142.

[9] Zhang, Yu.; Emma, O.; Yuwono, A.H.; Wang, J. Effect of Neodymium Doping on the Structure and Optical Properties of Mesoporous TiO_2 Thin Films. *Synthesis and Reactivity in Inorganic, Metal-Organic, and Nano-Metal Chemistry.* 38, 2008, 312-317.

[10] Huang, F.; et al. Optical parameters and absorption of copper (II)-azo complexes thin films as optical recording media. *Thin Solid Films.* 2005, 483, 251-256.

[11] Mahmoud, M.E.; Haggag, S.S. Surface layer-by-layer chemical deposition reaction for thin film formation of nano-sized metal 8-hydroxyquinolate complexes. *Polyhedron.* 2009, 28 181-187.

[12] El-Ghamaz, N.A.; El-Mallah, H.M. Optical properties studies on metal ligand bonding of novel quinoline azodyes thin films. *Solid State Sciences.* 2013, 22, 56-64.

[13] Houjou, H.; Kamurab, M. Striking effects of cobalt(III) nuclearity in fused salphen complexes on their electroconductivity and thin film transistor activity. *Organic Electronics*. 2013, 14, 3472-3476.

[14] Mahmoud, M.E.; Haggag, S.S. Nano-sized Co(II)-8-hydroxyquinolate complex thin film via surface layer-by-layer chemical deposition method: Optimized factors and optical properties. *Polyhedron.* 2009, 28, 3407-3414.

[15] Haggag, S.M.S.; Farag, A.A.M.; Mohamed, M.E. Layer-by-layer chemical deposition technique for thin film assembly of deposited nano-sized magnesium(II)-5,7-dinitro-8-hydroxyquinolate: Characterization and spectral–optical–electrical properties. *Polyhedron.* 2011, 30 2723-2732.

[16] Pattanaik, G R.; Pandya, D K. Layer-by-layer chemical deposition technique for thin film assembly of deposited nano-sized magnesium(II)-5,7-dinitro-8-hydroxyquinolate: Characterization and spectral-optical-electrical properties. *Thin Solid Films.* 2003, 433, 47-25.

[17] Faraga, A.A.M.; Haggag, S.M.S. Spectral–optical–electrical–thermal properties of deposited thin films of nano-sized calcium(II)-8-hydroxy-5,7-dinitroquinolate complex. *Spectrochimica Acta Part A.* 2011, 82, 467-474.

[18] Bulakhe, R.N.; Shinde, N.M.; Thorat, R.D. Deposition of copper iodide thin films by chemical bath deposition (CBD) and successive ionic layer adsorption and reaction (SILAR) methods. *Current Applied Physics.* 2013, 13, 1661-1667.

[19] Bai, H.; Ault, B.S. Infrared spectroscopic characterization of molecular complexes of dimethylcadmium with Group V and VI hydrides in inert matrices and cryogenic thin films. *Journal of Molecular Structure*. 1996, 377, 235-246.

[20] Galán, O. V.; Morales-Acevedo, A. Characterization of CBD-CdS layers with different S/Cd ratios in the chemical bath and their relation with the efficiency of CdS/CdTe solar cells. *Thin Solid Films*. 2007, 515, 6085-6088.

[21] Zaera, R.T.; Ryan, A.; Katty, A. Fabrication and characterization of ZnO nanowires /CdSe/CuSCN eta-solar cell. *C. R. Chimie*. 2006, 9, 717-729.

[22] Barwiolek, M.; Szlyk, E.; Surdykowski, A. New nickel(II) and copper(II) complexes with unsymmetrical Schiff bases derived from (1R,2R)(−)cyclohexanediamine and the application of Cu(II) complexes for hybrid thin layers deposition. *Dalton Trans*. 2013, 42, 11476-11487.

[23] Nakamoto, K. Infrared spectra of inorganic and coordination compounds, Front Cover. *New York: John Wiley & Sons*. 1963.

[24] Patil, C.D.; Jagadale, B.H.; Lokhande, A.D. Synthesis of polythiophene thin films by simple successive ionic layer adsorption and reaction (SILAR) method for supercapacitor application. *Synthetic Metals*. 2012, 162, 1400-1405.

[25] Wen, M.; Baolei, S.; Zhou, B.; Qingsheng, W. Controllable assembly of Ag/C/Ni magnetic nanocables and its low activation energy dehydrogenation catalysis. *J. Mater. Chem*. 2012, 22, 11988-11993.

[26] Xiang, J.; Li, J.; Zhang, X. Magnetic carbon nano fibers containing uniformly dispersed Fe/Co/Ni nanoparticles as stable and high-performance electromagnetic wave absorbers. *J. Mater. Chem.* 2014, 2, 16905-16914.

[27] Junling, G.; Xiaoling, W.; One-step seeding growth of controllable Ag@Ni core-shell nanoparticles on skin collagen fiber with introduction of plant tannin and their application in high-performance microwave absorption. *J. Mater. Chem*. 2012, 22, 11933-11942.

[28] Guojian, L.; Yongze, C.; Wangao, Q. Tenable phase formation in Ni-Fe thin films at nanoscale using high magnetic fields. *Vacuum*., 2014, 106, 75-78.

[29] Singh, A.K.; Deo, S.R.; Thool, G.S.; Singh, R.S. Synthesis and Characterization of Chemically Deposited Nanocrystalline CdSe Thin Film. *Synthesis and Reactivity in Inorganic, Metal-Organic, and Nano-Metal Chemistry*. 2011, 41, 1346-1350.

[30] Evans, R.C.; Douglas, P.; Winscom, C.J. Coordination complexes exhibiting room-temperature phosphorescence: Evaluation of their suitability as triplet emitters in organic light emitting diodes. *Coord. Chem. Rev*. 2006, 250, 2093-2126.

[31] Kumar., M.K. et al. Crystal growth, structural and optical properties of an organic ion-complex crystal: 4-N,N-dimethylamino-4-N-methylstilbazolium iodide. *Optik*. 2014, 125 5641-5646.

[32] Chen,. Z.; et al. Optical properties of nickel(II)–azo complexes thin films for potential application as high-density recordable optical recording media. *Solid State Communications*. 2007, 141, 1-5

[33] Hussien, M.A.A.; Nawar, H.N. Spectral characterization, optical band gap calculations and DNA binding of some binuclear Schiff-base metal complexes derived from 2-amino-ethanoic acid and acetylacetone. *Journal of Molecular Structure*. 2015, 1080, 162-168.

[34] Hosny, N.M.; Hussien, M.A.; Radwan, F.M. Synthesis, spectral characterization and DNA binding of Schiff-base metal complexes derived from 2-amino-3-hydroxyprobanoic acid and acetylacetone. *Spectrochimica Acta Part A: Molecular and Biomolecular Spectroscopy*. 2014, 132, 121-129.

Table. 1: The values of weight (w), thickness (d), maximal absorption values (Abs_{max}), absorption Wavelength (λ) and gap's energy (E_g**)** of Ni(II)-complexes thin films prepared on optimal conditions.

Complexes	**Concentration (M)**	**Cycle number**	**T (°C)**	**W (mg)**	**λ (nm)**	**Abs_{max}**	**d (µm)**	**E_g (eV)**
$[Ni(bpy)_3](SCN)_2$	10^{-2}	120	20	1.20	245	0.890	4,70	3.4
$[Ni\ (bpy)_3](Fe(CN)_5NO)$	10^{-2}	120	20	2.60	241	1.250	4,92	3.0
$[Ni(bpy)_3]\ ](Ag(CN)_2)_2$	10^{-2}	120	20	2.10	238	0.820	3,90	4.6

Fig. 1: The schematic depiction of successive ionic layer adsorption and reaction (SILAR) method.

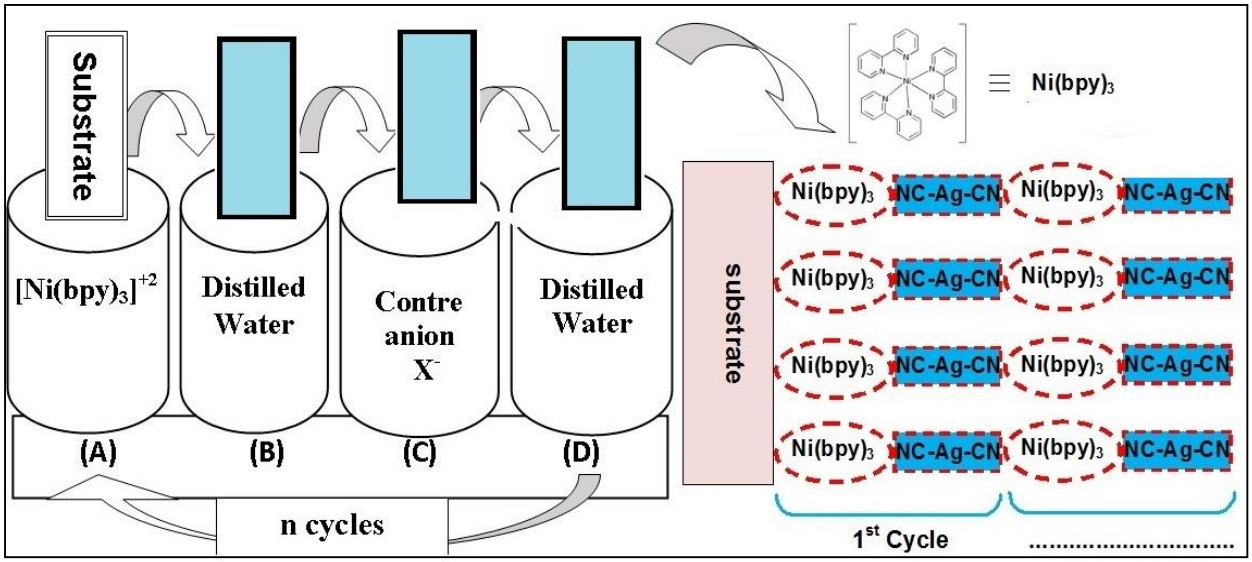

Fig. 2: Room temperature absorption spectra of Ni(II)-complexes thin films (A): [Ni(bpy)3](NCS)2, (B) $[Ni(bpy)_3](Fe(CN)_5NO)$, and (C): $[Ni(bpy)_3](Ag(CN)_2)_2$. And (D) report the variation of thin films thickness grows at (120 cycles and 20 °C) with different precursor's concentration.

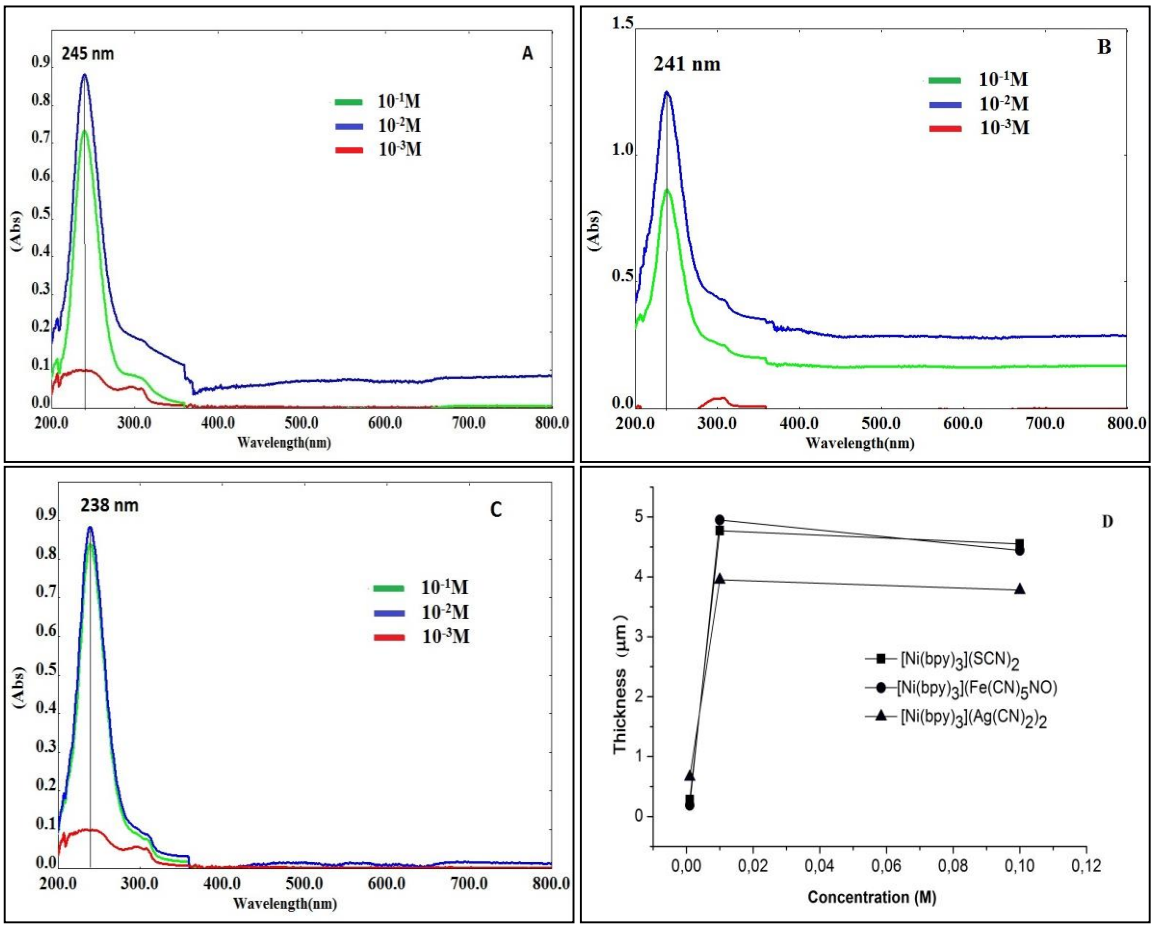

Fig. 3: Room temperature absorption spectra of Ni(II)-complexes thin films (A): $[Ni(bpy)_3](NCS)_2$, (B): $[Ni(bpy)_3](Fe(CN)_5NO)$ and (C): $[Ni(bpy)_3](Ag(CN)_2)_2$. (D) report the variation of thin films thickness grows at 20 °C and 10^{-2} M of precursors concentration with different cycles number.

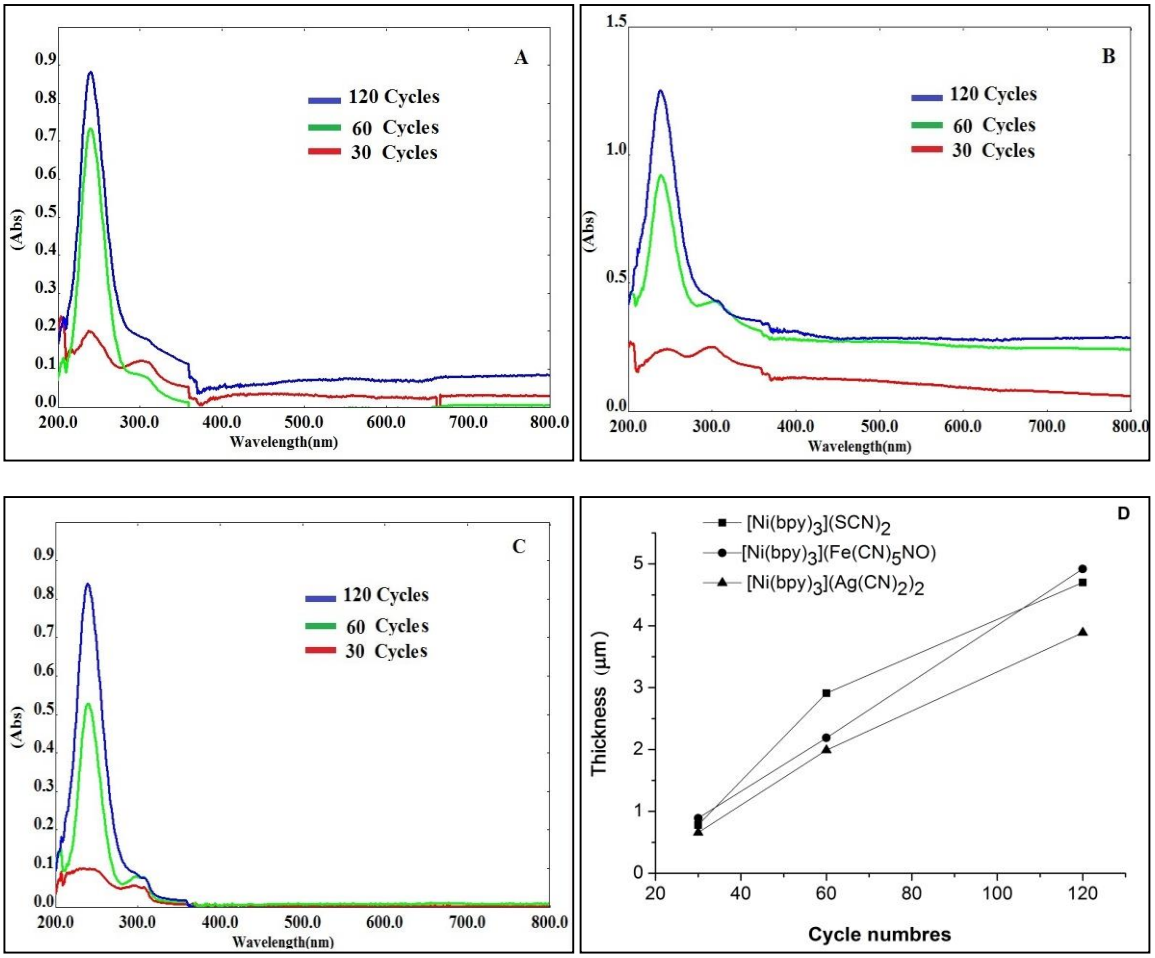

Fig. 4: Room temperature absorption spectra of Ni(II)-complexes thin films (A): $[Ni(bpy)_3](NCS)_2$, (B): $[Ni(bpy)_3](Fe(CN)_5NO)$ and (C): $[Ni(bpy)_3](Ag(CN)_2)_2$. (D) report the variation of thin films thickness grows at 120 cycles and 10^{-2} M of precursors concentration with different temperature.

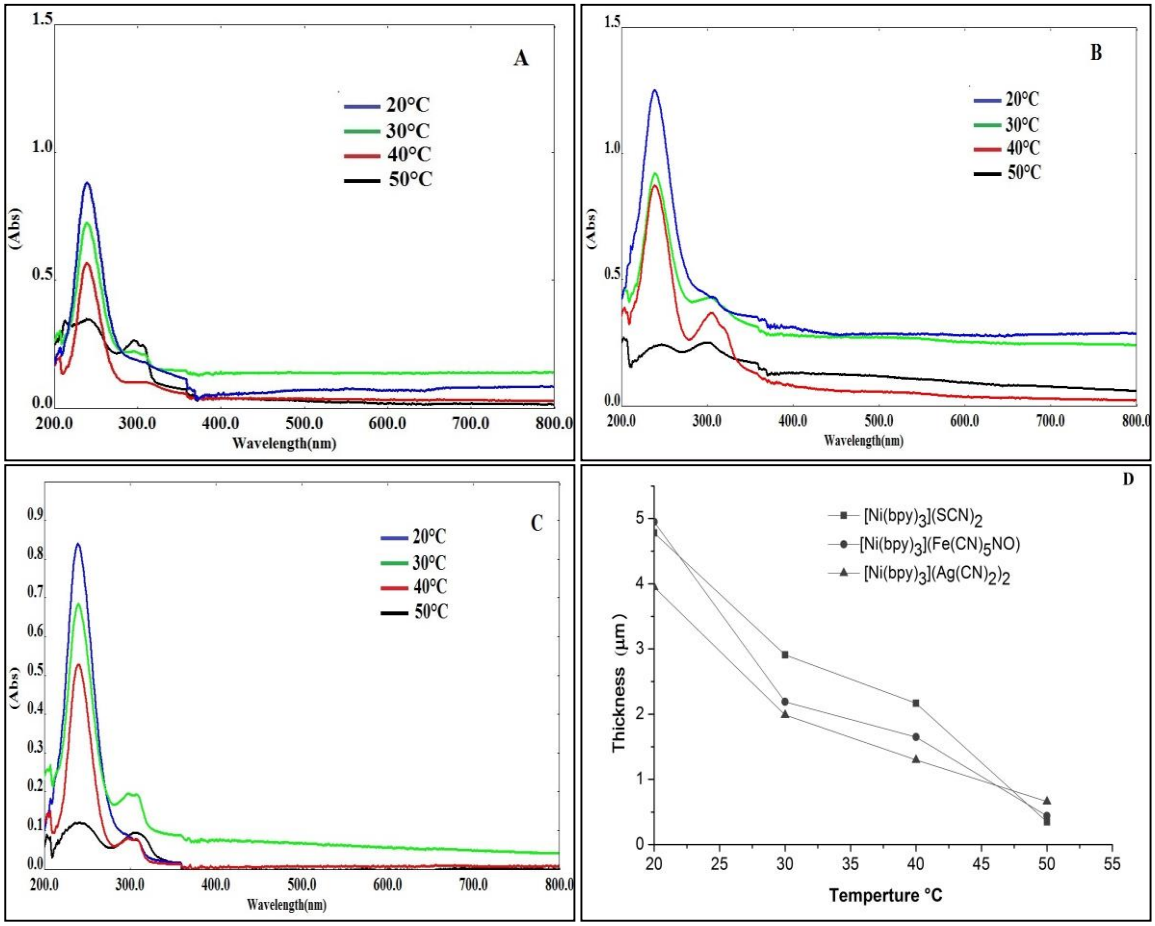

Fig. 5: Infrared spectra of Ni(II)-complexes thin film of A : $[Ni(bpy)_3](NCS)_2$, B: $[Ni(bpy)_3](Fe(CN)_5NO)$ and C: $[Ni(bpy)_3](Ag(CN)_2)_2$) grow at (20 °C, 10^{-2} M and 120 dipping cycles), using SILAR method.

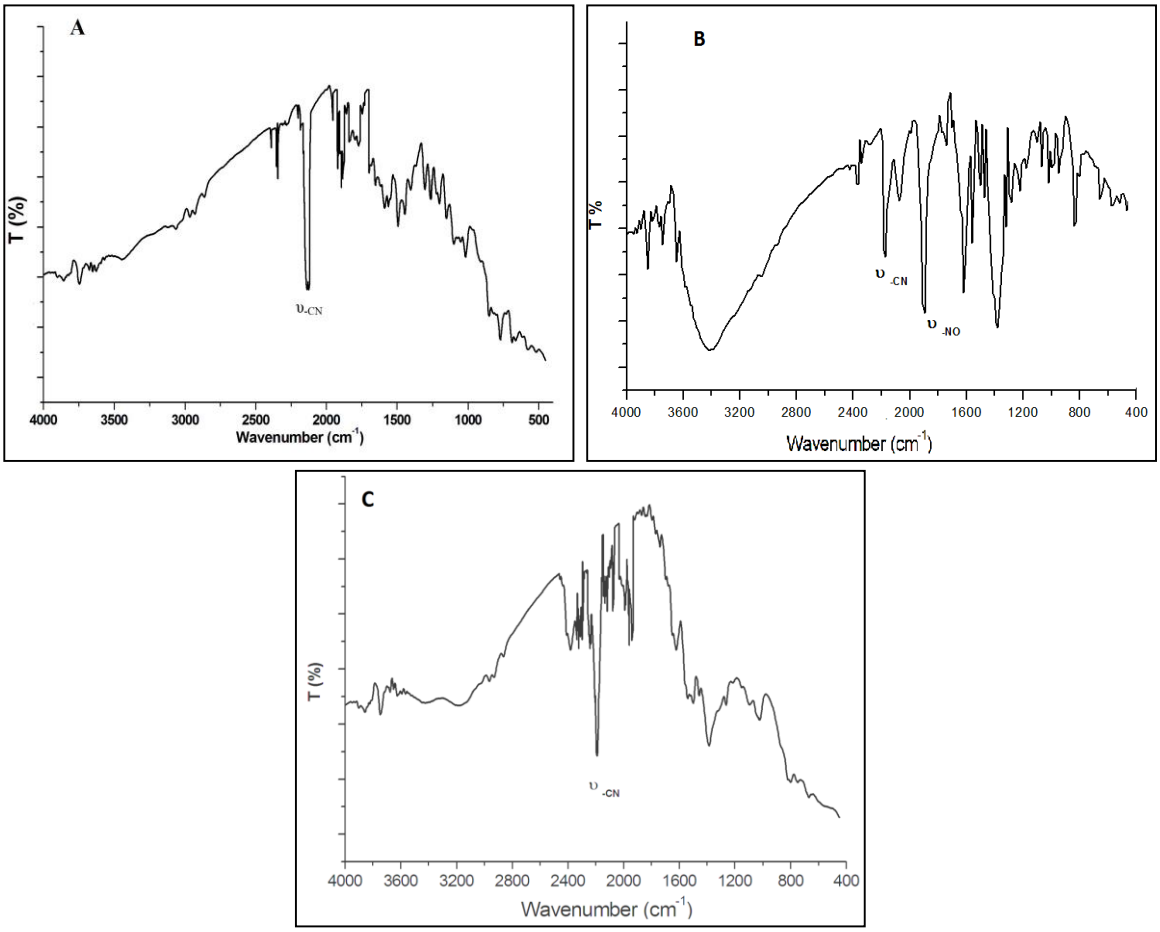

Fig. 6: DRX patterns of Ni(II)-complexes thin film of A : $[Ni(bpy)_3](NCS)_2$, B: $[Ni(bpy)_3](Fe(CN)_5NO)$ and C: $[Ni(bpy)_3](Ag(CN)_2)_2$) grow at (20 °C, 10^{-2}M and 120 dipping cycles) using SILAR method.

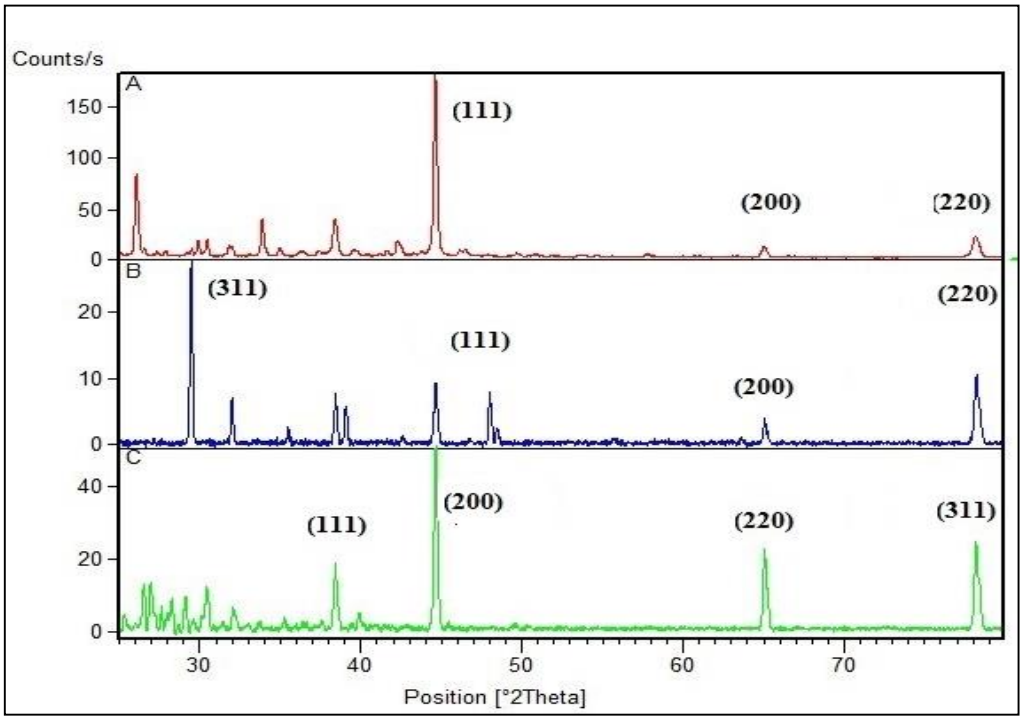

Fig. 7: The SEM micrographs of Ni(II)-complexes thin film of A: $[Ni(bpy)_3](NCS)_2$, B: $[Ni(bpy)_3](Fe(CN)_5NO)$, and C: $[Ni(bpy)_3](Ag(CN)_2)_2$ grows at (20°C, 10^{-2} M and 120 dipping cycles) using SILAR method.

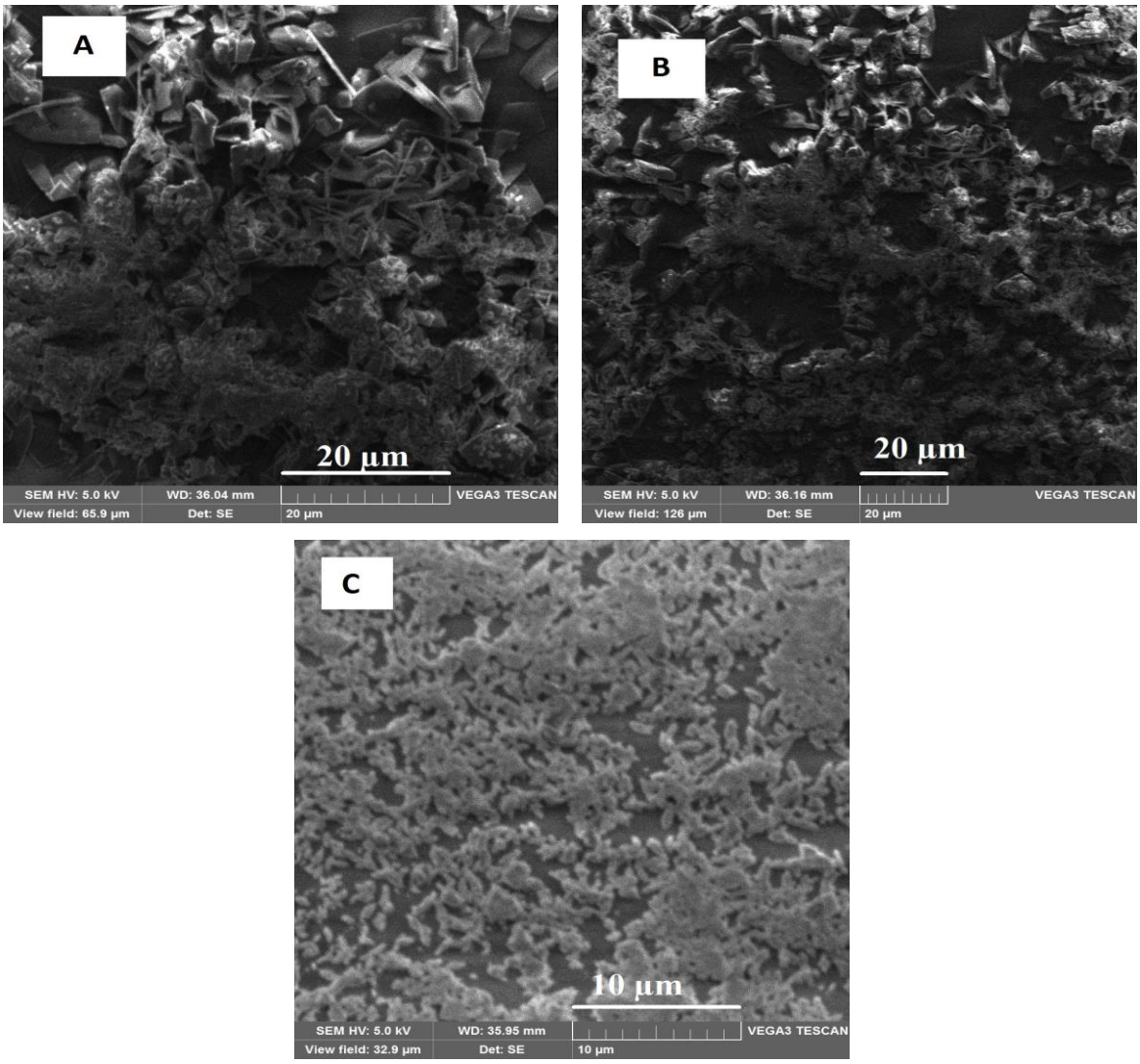

Fig. 8: Plot of absorption coefficient (α) and $(\alpha h\upsilon)^2$ verses photon energy of $[Ni(bpy)_3](SCN)_2$ thin film deposed on glass substrate using SILAR method.

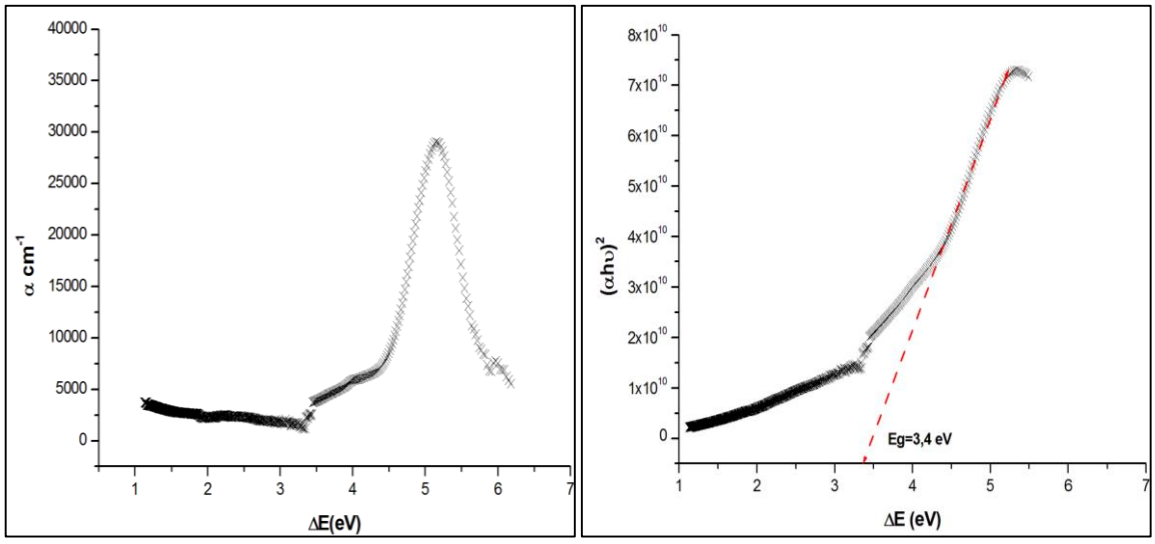

Fig. 9: Plot of absorption coefficient (α) and $(\alpha h\upsilon)^2$ verses photon energy of $[Ni(bpy)_3](Fe(CN)_5NO)$ thin film deposed on glass substrate using SILAR method.

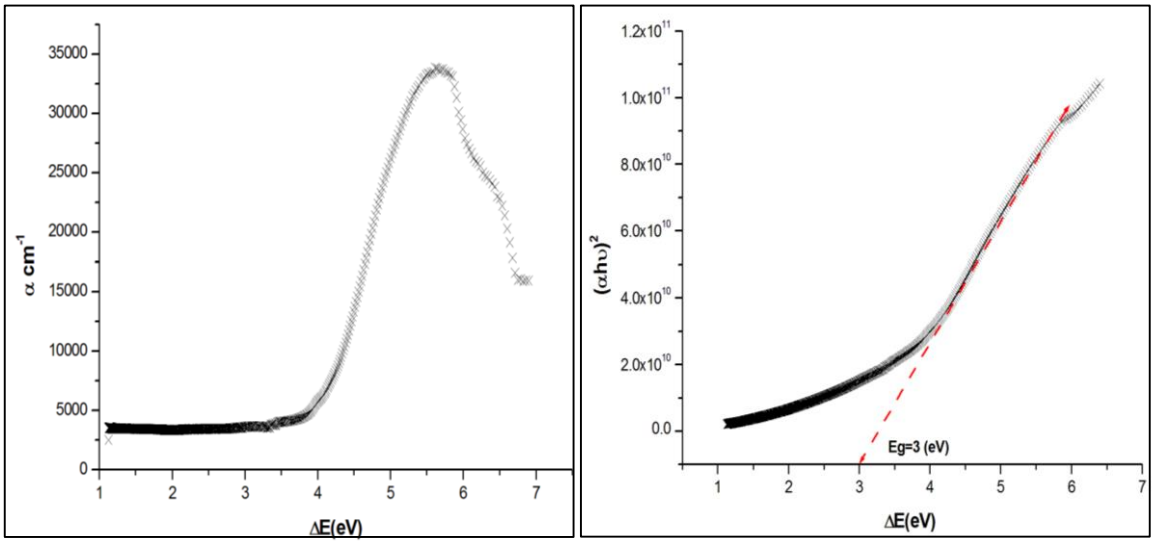

Fig. 10: Plot of absorption coefficient (α) and $(\alpha h\upsilon)^2$ verses photon energy of $[Ni(bpy)_3](Ag(CN)_2)_2$ thin film deposed on glass substrate using SILAR method.